

FINITE ELEMENT METHOD ANALYSIS OF NON – LINEAR BEHAVIOUR OF IMPLANTS AND STENTS.

J. Awrejcewicz, M. Ciach, K. Włodarczyk

Division of Automatics and Biomechanics
Technical University of Lodz
1/15 Stefanowski St., 90-924 Lodz, POLAND
e – mail: awrejcew@ck-sg.p.lodz.pl

Keywords: FEM, Stents, Non-linear Plasticity, Intervertebral Disc Implants, Hyperelastic Mooney – Rivlin Non – Linear Material Constitutive Laws, Kinematics Strain Hardening.

Abstract. *Both artificial intervertebral disc implant in the human spinal segment body to the natural intervertebral disc and the intracoronary stents in ischaemic heart disease are analysed. In the first case the created numerical model involved the application of hyperelastic Mooney-Rivlin non-linear material constitutive laws. The constants for the strain energy density function have been evaluated from the experiment performed on biocompatible, hydrophilic, radiolytically polymerised and crosslinked vinyl pyrrolidone (VP). In the second case, stents implanted with the use of a balloon have been analysed. A very interesting fact of the implanting is that during the expanding the boundary of plasticity is exceeded, the material is hardened and the whole construction still works in the expanding state. Special software, the program of the Finite Elements Method ANSYS, was used to create the numerical model. Several stages leading to full expansion of a stent were taken into consideration during modelling. The constructed model exhibited a non-linear character because of non-linear straining as well as non-linear formula making use of plasticity criterion according to von Mises, and of kinematics strain hardening of the materials. This model aims at taking into consideration the history of deformations, what has an enormous influence upon the level of deformations and final stresses, caused by the vessel interaction upon the implant, and what follows is the definition of stent fatigue strength during the millions of cycles caused by heart action. Surgery steel 316L has been accepted as the material from which the mentioned above stent has been made.*

1. INTRODUCTION

As it has been earlier mentioned we focus on numerical construction of the intervertebral disc implant and the stent.

The intervertebral discs make up about one fourth of the entire length of the vertebral column. The discs absorb the stress and strain transmitted to the vertebral column. One of the most common problems faced recently in medical practice is the clinical complication of the intervertebral disc degeneration. The degeneration of discs is a complex process that involves variations in the composition and function of the disc. Some of those regressive changes are connected with ageing process making the problem nearly universal [1-4]. This destructive process most frequently is observed as spondylosis, which is an after-effect of disc herniation and bony spurs familiar to osteophytes. Both osteophytes and disk herniations may expand the intervertebral foramina and vertebral canal causing compression acting on nerve roots and the spinal cord, respectively. This may result in severe pain, dysfunction and disability including weakness and paresis of upper and lower limbs. The compression acting on spinal root results in pain radiating across the back of the shoulder, arm and down to forearm and fingers. The spinal cord compression is responsible for progressive weakness of lower and upper limbs that leads to complete disability when untreated. Surgical treatment is employed in those cases when pain does not respond to conservative management and when neurological deficits are developed. Surgical intervention relieves pain and prevents permanent disability caused by neurological deficits. A number of operative procedures have been utilized to relieve compression of the cervical spinal cord and nerve roots caused by a disc disease. However, most of them involve stabilisation of the injured spinal segment using different fixation systems. Those procedures relieve pain connected with the compression of the spinal cord but at the same time after fusion (arthrodesis), fused vertebrae do not perform in the structure of the spine the same role of the motion segment as it is in an intact spine. In the paper the authors constructed the numerical model of an artificial intervertebral disc (Fig.1). Numerical analyses involved the application of Finite Element Method using commercially available application – Ansys 5.4. For the numerical model, hyperelastic Mooney-Rivlin constants have been determined from experimental tests. Steady state numerical investigations have been further compared with results of the dynamical analysis.

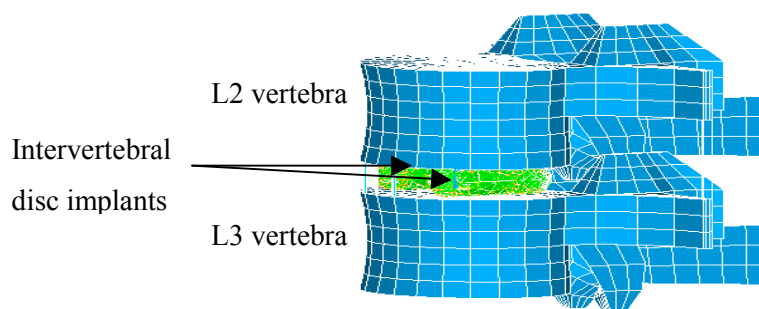


Fig. 1. The application of the intervertebral disc implant in the L2-L3 lumbar spine segment

In the second case the research is oriented towards a stent application.

Heart is the organ the work of which can be compared with the mechanism of the pump. Its task is to deliver blood to all parts of the body. Blood is delivered to myocardium through blood vessels called coronary arteries. In case of coronary arteries disease which is caused by cholesterol deposition the arteries can be narrowed or there may occur artery occlusion. The decrease of blood flow causes the myocardial hypoxia. It results in the sharp pain in the thorax. Many tests are conducted in order to discover the illness. Myocardial catheterization - coronaro-graphy – is the most important diagnostic method [5]. The method is based on introducing a thin tube called catheter to the outlet of coronary vessels by puncturing the skin and the vessel in the groin or in the forearm. The catheter enables the doctor to inject a special liquid (contrast) to a sick vessel, and to observe the shape and size of coronary vessels by means of X-ray apparatus [6]. Based on this examination the doctor can estimate the flow in the vessel, and whether there are occlusions which might cause coronary disease occurring in people at different ages. The flow occlusion in the vessels leads to necrosis of a certain area of myocardium called myocardial infarct. Then the sick person feels sharp pain in the thorax. Coronary disease can occur in people at different ages. Its symptoms considerably decrease life activity. There are many ways of curing myocardial ischemia. One of these is the implantation of one or a few stents into the coronary vessel. A stent is a kind of scaffolding which is implanted in the critically narrowed section in order to support the walls of the vessel and to broaden its light [6].

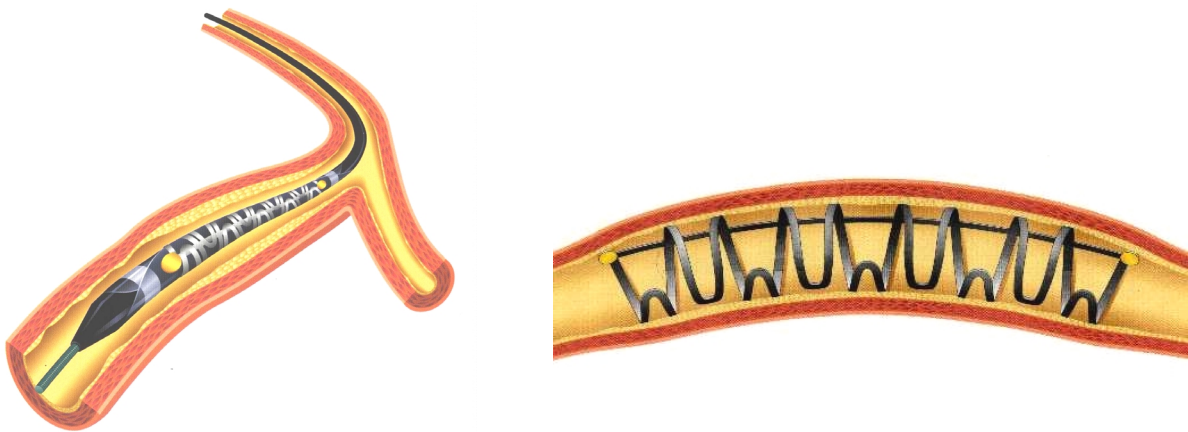


Fig.2. Stent GR II (Cook) [7, 8]

The aim of the following study is to create a numerical model showing the stage of stent expansion, interaction of blood vessel upon the stent, what will allow to determine the value of straining and stress, and the fatigue resistance of the stent.

2. FINITE ELEMENT MODEL OF THE INTERVERTEBRAL DISC IMPLANT

In order to analyse the behaviour of the intervertebral disc implant an appropriate FEM model has been constructed. For the purposes of the investigation, the former model of an intact spinal segment has been consequently adopted [1-4]. Geometry and diameters of the artificial intervertebral disc implant have been the same as for a real model constructed by the authors [9]. To approximate the structure of the human intervertebral disc the pair of cylinder shaped implants has been utilised. To simplify the numerical solution and to reduce the time of numerical analysis, the homogenous material has been used to approximate the solid of the artificial intervertebral discs.

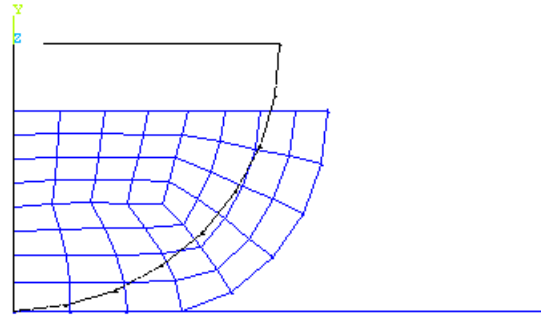


Fig. 3. Numerical model representing the structure of the artificial intervertebral disc

Additionally, to obtain the results for the model, only a quarter of one of the cylinders was a subject of numerical investigations with respect to the double symmetry of the structure (see Fig. 3).

Numerical investigation involved the application of hyperelastic material properties. The material is said to be hyperelastic if there exists a scalar function of one of the strain or deformation tensors, whose derivative with respect to a strain component determines the corresponding stress components [10]. This formula can be expressed by

$$S_{ij} = \frac{\partial W}{\partial E_{ij}} \equiv 2 \frac{\partial W}{\partial C_{ij}}, \quad (1)$$

where: S_{ij} - components of the second Piola-Kirchhoff stress tensor, W - strain energy function per unit undeformed volume, E_{ij} - components of the Lagrangian strain tensor, C_{ij} - components of the right Cauchy-Green deformation tensor.

The Mooney-Rivlin constitutive laws representing the stress-strain relationship have been adopted. For the model the Mooney Rivlin strain energy density function has the following form:

$$W = a_{10} (I_1 - 3) + a_{01} (I_2 - 3) + \beta (I_3^2 - I_3^{-2})^2, \quad (2)$$

where:

I_i – reduced strain invariants in the i^{th} direction,

$$I_1 = I_1 I_3^{-1/3},$$

$$I_2 = I_2 I_3^{-2/3},$$

$$I_3 = I_3^{1/2},$$

a_{10}, a_{01} – Mooney-Rivlin material constants

$$\beta = \frac{(1 + \nu)a_{10} + a_{01}}{24(1 - 2\nu)},$$

ν - Poisson's ratio

I_i – invariants of Cauchy-Green's deformation tensors

$$I_1 = C_{ii}, I_2 = 1/2(I_1^2 - C_{ij}C_{ij}), I_3 = \det C_{ij}.$$

In order to find the Mooney-Rivlin constants a_{10}, a_{01} , an axial compression test on the biocompatible, hydrophilic, radiolytically polymerized and crosslinked vinyl pyrrolidone (VP) has been performed. From the experiment the following strain-stress dependency have been utilised in the numerical analysis (Fig. 4).

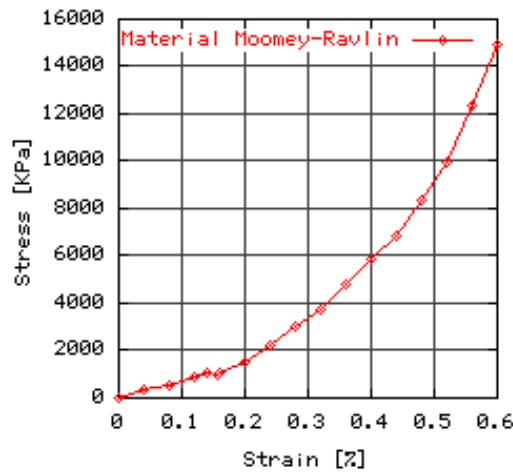


Fig. 4. Stress-Strain dependency in the axial compression tests required to obtain the Mooney-Rivlin constants

Axial loads have been applied twice to the model of the implant. Firstly, the steady state numerical analysis of the intervertebral disc implant has been performed. The results of that analysis have been compared with the results of numerical and experimental tests of an intact human lumbar spine. Additionally, transient dynamical analysis involved the application of

the dynamic loading. The basic equation of motion in the transient dynamic analysis can be expressed as:

$$[M]\{\ddot{u}\} + [C]\{\dot{u}\} + [K]\{u\} = \{F(t)\}, \quad (3)$$

where:

$[M]$ – mass matrix, $[C]$ – damping matrix, $[K]$ – stiffness matrix, $\{\ddot{u}\}$ – nodal acceleration vector, $\{\dot{u}\}$ – nodal velocity vector, $\{u\}$ – nodal displacement vector, $\{F(t)\}$ – load vector.

At any given time t these equations can be thought as a set of “static” equilibrium equations that also take into account inertia forces ($[M]\{\ddot{u}\}$) and damping forces ($[C]\{\dot{u}\}$).

In the steady state analysis the load has been applied progressively to the value of 6000 N. In transient dynamic analysis, the load has been applied in the time of 0.2 s to the value of 1000 N (concerning only a quarter of the cylinder) and then, additionally, sinusoidal loading has been accomplished.

The results of the static numerical analysis have been compared with the former numerical simulations accomplished by authors, and other experimental investigations performed on the human lumbar spinal segment. In Fig. 5 the results in the form of the axial compression test vs displacement show significant correspondence of the numerical results of the analysis of artificial intervertebral discs with the results (numerical and experimental) accomplished for an intact intervertebral disc.

Additionally two dynamical analyses have been performed. First, to the compared statical and dynamical approach to the body of the implant, the same load as for the static analysis has been applied in time of 0.2 s. The second stage of investigation involved the application of the sinusoidal load in time of one second. Graphs in Figs. 5 to 7 show consequently comparison of the statical and dynamical analysis, load history for the model of the implant and corresponding to the load displacement in a diametrical direction of the implant under axial compression tests.

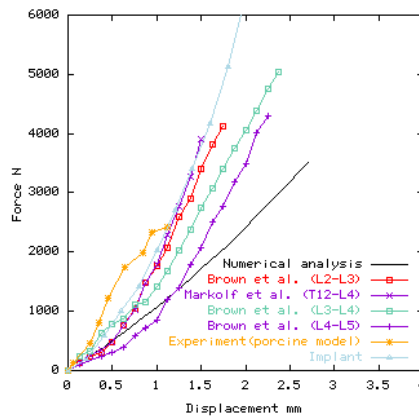


Fig. 5. Static test of artificial and intact intervertebral discs

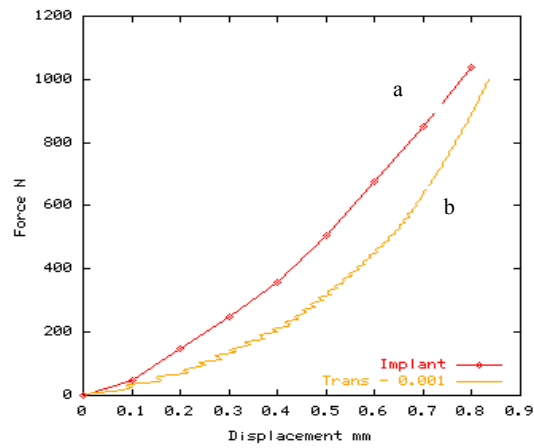


Fig 6. The comparison of steady state: a) and dynamical results: b) of axial compression tests performed on the model representing the intervertebral disc implant

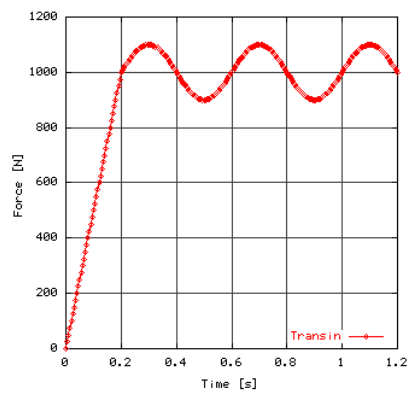


Fig. 7. Load history graph of the sinusoidal loading of the model of the implant

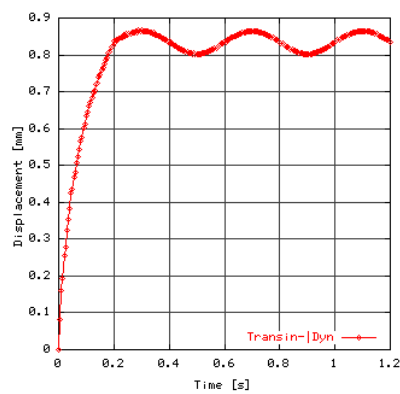


Fig. 8. Displacement in time corresponding to the load from Fig. 6

3. STENTS

Stents are made of metal rustless net. The stent looks like a thin tube before it is introduced into the vessel. Once there, it is expanded to the size of the vessel in which it has to be placed. The flexibility enables leading the stent through the bends of proximate sections of coronary vessels, and implanting it into the occluded part. The lack of crushing susceptibility of the open stent diminishes the cycling stretching of the vessel wall. Materials used for stent construction differ in thrombus properties. Biologically indifferent rustless steel marked 316L is most frequently used for stent production. It is very important to minimize the surface thickness and porosity of metal. Rustless steel is characterized by long durability – and this is why only a small amount of steel is sufficient for the production of a stent. Small weight of a steel, however, is hardly visible in fluoroscopy, it hinders on the one hand precise location of a stent, on the other hand its recognition in case of displacement.

Carefully chosen size of a stent (the ratio of the diameter to the diameter of the vessel is from 1 to 1,1) determines the success of the implantation. On the one hand the stent narrower than the size of the vessel tends to migrate, on the other hand the excessive expansion of the walls causes the damage of the inner and central layer of the artery.

At present there are 3 basic types of stents as regards the method of implanting and the material used:

- Stents implanted by the use of the balloon – they were introduced by J. Palmaz in 1984. The use of the balloon makes the advantage of the plastic properties of rustless steel and enables precise installation of a stent. A low profile and a small surface of the metal is the advantage of this kind of the stent. The stent once expanded above the plastic properties of the steel does not change its shape. Palmaz-Schatz, Gianturco-Rubin, Wiktor and Strecker stents are of this type. New models are the stents: Crown, Cross, Flex, XT, Freedom, NIR, Angiostent and Multi-Link [10].
- Self expanding stents - built from elastic spiral of nitinol, which, having self expanded, can take different shapes, preserving all the time centrifugal expanding force, e.g. Wallstent. Flexibility at introducing and stability after implanting are the advantages of Wallstent. In spite of these advantages and results presented by U. Sigwort multicenter clinical testing showed that Wallstent is characterized by higher risk of thrombosis.
- Stents expanding under the influence of heat. A stent of this kind built of nitinol spiral (the alloy of nickel and titanium) is placed on the catheter of low profile. The stent being introduced into the occluded place and heated, the metal spiral expands to the required dimension. The complicated process of introduction, and hard to foresee degree of expansion of nitinol stent restrict its clinical interest.

Stents implanted with the use of a balloon have been situated in the centre of our interests. A very interesting fact during the implanting is that during the expanding the boundary of plasticity is exceeded, the material is hardened and the whole construction still works in the expanding state. Special software – the programme of the Method of Finite Elements ANSYS was used to create the numerical model (see Fig. 9).

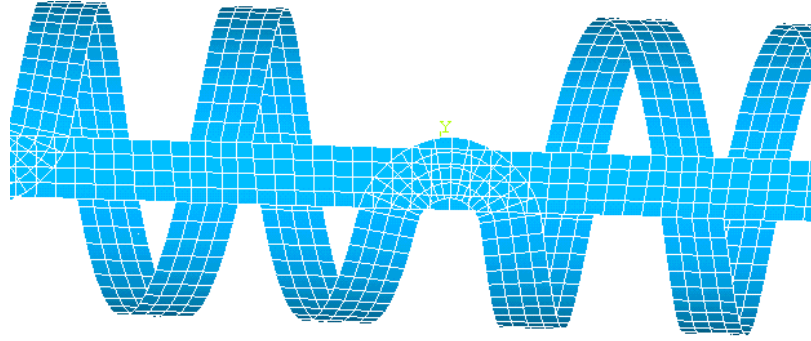


Fig.9. Numerical model of the stent divide into finite elements

Several stages leading to full expansion of stent were taken into consideration during modelling. The constructed model has got as nonlinear character because of nonlinear straining as well as nonlinear formula making use of plasticity criterion according to von Misses, and of kinematic strain hardening of the materials. The equivalent plastic stress σ_e is defined by:

$$\sigma_e = \left[\frac{3}{2} (\{s\} - \{\alpha\}^T) \cdot [M] (\{s\} - \{\alpha\}) \right]^{\frac{1}{2}}, \quad (4)$$

where:

$$\{s\} = \{\sigma\} - \sigma_m [111000]^T, \quad (5)$$

$\{s\}$ – vector of stress deviator, $[M]$ – matrix describing plastic stress changes, $\{\alpha\}$ – translation vector of plastic deformation, σ_m - hydrostatic stress = $\frac{1}{3}(\sigma_x + \sigma_y + \sigma_z)$.

The whole model vessel-stent is built of 3.273 elements. The stent was modelled from elements of SHELL 93 type (spatial, 8 – nodal), and the vessel from the elements of CONTA 170 and CONTA 174 type (spatial, 8 – nodal) - see Fig. 10.

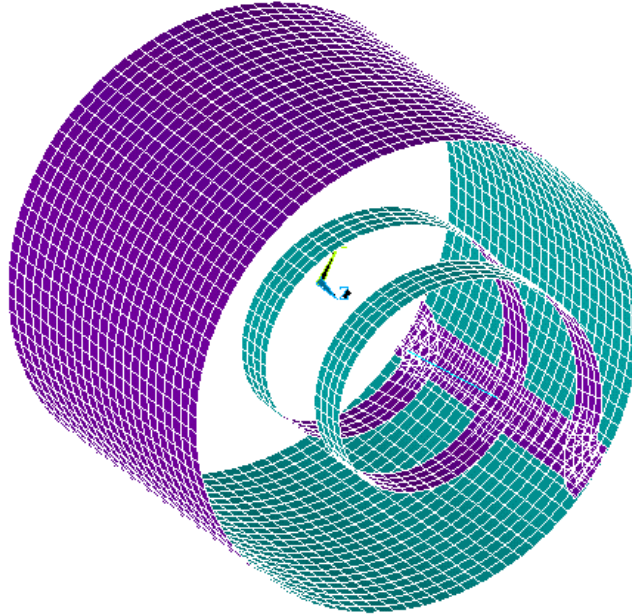


Fig. 10. Numerical model vessel-stent with the division into the finite elements

The following several stages of numerical simulation occur:

- the stent is expanded by the inner pressure $p=6\text{atm}$,
- the initial stage takes place in the linear elastic range (Hooke's law), small deformations,
- next the final results of elastic stage stresses are the initial conditions of the plastic stage and the physical law takes the form of (4) (large non-linear deformations),
- stent becomes totally expanded (touches the surface of the vessel, the material becomes hardened),
- the vessel begins to press the stent periodically with the pressure $p=250\text{ mm Hg}$ (the safety margin has been accepted). The pressure of interaction vessel – stent is about $p=83,9\text{ mm Hg}$ [11].

The above model aims at taking into consideration the history of deformations, what has an enormous influence upon the level of deformations and final stresses, caused by the vessel interaction upon the implant, and what follows is the definition of stent fatigue strength during the millions of cycles caused by heart action. Surgery steel 316L has been taken as the material from which the mentioned above stent has been made.

The data concerning the level of deformations and stresses in particular stages of stent expansion have been obtained as a result of numerical calculations. Figure 11 shows the exemplary results of reduced stress achieved for elastic and plastic stage.

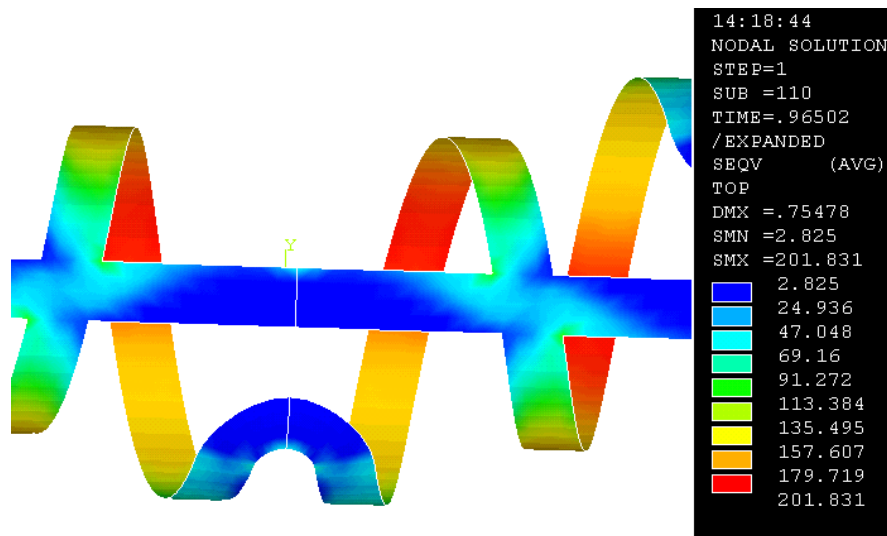


Fig.11. Reduced stresses – plastic stage

4. CONCLUDING REMARKS

Several conclusions can be drawn from the above investigation. The hyperelastic Mooney-Rivlin material seems to be very applicable to describe the behaviour of materials used to construct artificial intervertebral discs. Additionally, axial compression numerical tests of the artificial disc of the presented material constitutive laws show significant correspondence to intact intervertebral discs.

The dynamical analysis of an implant display larger displacements in the model than the static tests. The reason for this behaviour are additional inertia forces ($[M]\{\ddot{u}\}$) presented in the model. Thus this is very important to remember about a significant role of the dynamics while considering the biomechanical behaviour of the human vertebral column.

The use of numerical methods and computer techniques for modelling of the phenomena occurring in the human body are getting more and more popular and give better and better results. In the case of examinations of human heart numerical simulations are sometimes the only ones that can be carried out. In the case of coronary stents they allow to define the level of stress and deformation, and what follows – fatigue resistance. Computer simulation gives the scientists the information that can be useful while getting the optimal shape in construction of implants. Then the implant constructed in this way is subject to testing on fatigue machines, on animals, and then implanted to human coronary vessels. The cost of numeric simulations, however, cannot be compared to other kinds of investigation.

REFERENCES

- [1]Awrejcewicz J., Ciach M., Kleiber M. (Eds.), Proceedings of the conference on "Biomechanics - modelling, computational methods, experiments and biomedical applications", Lodz, December 7-8, 1998.
- [2]Bedzinski R."Engineering biomechanics, the chosen problems", Wroclaw Technical Univ. Press, Wroclaw, 1997.
- [3]Ciach M., Awrejcewicz J., "Finite element analysis and experimental investigations of the intervertebral disc in the human and porcine lumbar spinal segment", Proceedings of the Conference on "Biomechanics - modelling, computational methods, experiments and biomedical applications", Lodz, December 7-8, pp 53-64, 1998.
- [4]Ciach M., Awrejcewicz J., "Numerical analysis and Experimental Investigation of Intervertebral disc in human lumbar and Cervical Spinal Segment", XXXVIII Symposium, "Modelling in Mechanics", February 8-12, pp 53-58, 1999.
- [5] Brzostek T., "Stents in ischaemic heart disease", Polish Cardiology N 45,1996, pp 541-547.
- [6] Medical University in Lodz, "Materials concerning stents implanting", Lodz, 1998.
- [7] GR II Coronary Stent – Reference Manual, COOK Cardiology, 1998.
- [8] GR II Coronary Stent – Correct Sizing, COOK Cardiology, 1998.
- [9]Stasica P., Rosiak J., Ciach M., Radek M., "Approach to construct hydrogel intervertebral disc implants – experimental and numerical investigations", International Congress of Biomaterials, 30.05-02.06, Krakow, 1999.
- [10] Khonke P. (Ed.), ANSYS Theory Reference, Release 5.4, Canonsburg, 1994.
- [11] Brazenor R.M. and Angus J.A."Ergometrine contracts isolated canine coronary arteries by a serotonergic mechanism", Journal Pharmacol. Exp., Nr 218, pp 530-536, 1981.